

Estimating the “Effective Period” of Bilinear Systems with Linearization Methods, Wavelet and Time-Domain Analysis: From Inelastic Displacements to Modal Identification

Nicos Makris¹ and Georgios Kampas²

¹Professor, Dept. of Civil Engineering, University of Patras, Greece, GR 26500, nmakris@upatras.gr

²Civil Engineer, Robertou Galli 27, Athens, Greece, GR 11742, geekampas@gmail.com

ABSTRACT

This paper revisits and compares estimations of the effective period of bilinear systems as they result from various published equivalent linearization methods and signal processing techniques ranging from wavelet analysis to time domain identification. This work has been mainly motivated from modal identification studies which attempt to extract vibration periods and damping coefficients of structures that may undergo inelastic deformations. Accordingly, this study concentrates on the response of bilinear systems that exhibit low to moderate ductility values (bilinear isolation systems are excluded) and concludes that depending on the estimation method used, the values of the “effective period” are widely scattered and they lie anywhere between the period-values that correspond to the first and the second slope of the bilinear system. More specifically, the paper shows that the “effective period” estimated from the need to match the spectral displacement of the equivalent linear system with the peak deformation of the nonlinear system may depart appreciably from the time needed for the nonlinear system to complete one cycle of vibration. Given this wide scattering the paper shows that for this low to moderate ductility values (say $\mu < 10$) the concept of the “effective period” has limited technical value and shall be used with caution and only within the limitations of the specific application.

Keywords: Modal Period, Equivalent Linear Analysis, System Identification, Time-Frequency Analysis, Yielding Structures, Statistical Linearization.

1. INTRODUCTION

The development of an equivalent linear system that approximates the maximum displacement of a bilinear hysteretic system when subjected to dynamic loading goes back to the seminal work of Caughey [1],[2]. By that time the elastic response spectrum was well developed and understood, and had become a central concept in earthquake engineering (Chopra [3] and references reported therein). Once available, the main attraction of the elastic response spectrum is that it offers the most significant features of the structural response without requiring knowledge of the time history of the excitation; while, its limitation is that it is defined only in relationship to elastic structures. Starting in the late 1950s researchers began recognizing the importance of studying the response of structures deforming into their inelastic range and this led to the development of the inelastic response spectrum (Veletsos and Newmark [4], Veletsos et al. [5], Veletsos and Vann [6]).

In parallel with the development of inelastic response spectra in earthquake engineering, there has been significant effort in developing equivalent linearization techniques (Caughey [1],[2], Rosenblueth and Herrera [7], Roberts and Spanos [8], Crandall [9], among others) in order to define equivalent linear parameters (natural periods and damping ratios) of equivalent linear systems that exhibit comparable

response values to those of the nonlinear systems. While the initial efforts in developing equivalent linearization techniques originated in the fields of random vibration and structural mechanics, these techniques found gradually major applications in earthquake engineering.

One of the major challenges in earthquake engineering is the estimation of the peak inelastic deformation of yielding structures. Traditionally, seismic design has not been carried out with nonlinear time-history analysis; instead, seismic deformation demands are established with the maximum response of “equivalent” linear single-degree-of-freedom (SDOF) systems via the use of linear elastic response spectra. Thus, through the years various displacement base methods (Miranda and Ruiz-Garcia [10] and references reported therein) have been proposed to estimate the maximum inelastic displacements from the maximum displacement of equivalent linear elastic SDOF systems. Accordingly, in earthquake engineering the main goal when developing an equivalent linear system is that the peak elastic deformation, is comparable to the peak deformation of the inelastic system. Nevertheless, this exercise does not assure that these two “equivalent” systems will also have comparable vibration characteristics –that they will need the same time to complete a one vibration cycle.

Early studies on estimating the effective period of bilinear systems by comparing peak spectral values when subjected to earthquake loading were published by Iwan and Gates [11] and Iwan [12] after minimizing the root mean square (RMS) of the difference between the spectral displacements of a bilinear system and a family of potentially equivalent linear systems. Some 35 years later, Guyader and Iwan [13] revisited this problem and offered refined expressions for a conservative estimation of the effective period and damping of a class of yielding systems. Recently Giaralis and Spanos [14] returned to the framework of stochastic equivalent linearization technique and presented a methodology to derive a power spectrum which, while represents a Gaussian stationary process it is compatible in a stochastic sense with a given design spectrum. This power spectrum is then treated as the excitation spectrum to determine the effective period and damping coefficient of the corresponding equivalent linear system.

In the abovementioned “spectral” studies, the effective period of the equivalent linear system is determined by minimizing the difference (error) of either the response spectra (Iwan and Gates [11], Iwan [12], Guyader and Iwan [13]), or the response histories of the nonlinear and the equivalent linear systems (Giaralis and Spanos [14]). While the estimation of inelastic deformations has a central role in the performance of earthquake resistant structures, the identification of vibration characteristics of yielding structure is also receiving increasing attention mainly due to the growing need for monitoring the structural health of civil infrastructure. Accordingly, within the context of system identification, the effective period of a yielding system may be understood as the prevailing vibration period (time needed to complete one vibration cycle) of the response history and can be extracted with signal processing methods which examine the response signal alone. The performance of these methods is also assessed in this study in an effort to conclude whether the “effective” period that is estimated in order to estimate inelastic displacement is a representative vibration period of the inelastic system.

By the mid 1980s wavelet transform analysis had emerged as a unique new time-frequency decomposition tool for signal processing and data analysis (Grosman and Morlet [15]). At present, there is a wide literature available regarding its mathematical formulation and its applications (Mallat [16], Addison [17], Newland [18] and

references reported therein). Given that wavelets are simple wavelike functions localized in time they emerge as a most useful tool for extracting the dominant period of the response of bilinear systems.

In parallel with the wavelet transform analysis, various powerful time-domain methods have been developed and applied successfully to extract the dominant period of signals. One of the most well known and powerful methods for linear systems in the system identification community is the Prediction Error Method (PEM). It initially emerged from the maximum likelihood framework of Aström and Bohlin [19] and subsequently was widely accepted via the corresponding MATLAB [20] identification toolbox developed following the theory advanced by Ljung [21], [22], [23].

In this work the prediction error method is also employed to extract the dominant effective period of the response of bilinear hysteretic systems and the results obtained from this time domain method are compared with the results obtained with the above-mentioned time-frequency analysis (wavelet transform) and the equivalent linearization methods also introduced in this section.

2. SIMPLE GEOMETRIC RELATIONS

The most elementary concept of an effective period of a system with bilinear behavior is the period associated with K_{eff} , that is the slope of the line that connects that axis origin with the point on the backbone curve where we anticipate the maximum displacement, u_{max} , to occur. This concept of a secant stiffness was apparently first proposed by Rosenblueth and Herrera [7] and then received wide acceptance for the estimation of maximum inelastic displacement of yielding structures [Miranda and Ruiz Garcia [10] and references reported therein).

With reference to Figure 1 one can derive via the use of similar triangles a relation between the effective stiffness, K_{eff} and the first slope of the bilinear model, K_1 .

According to Figure 1,

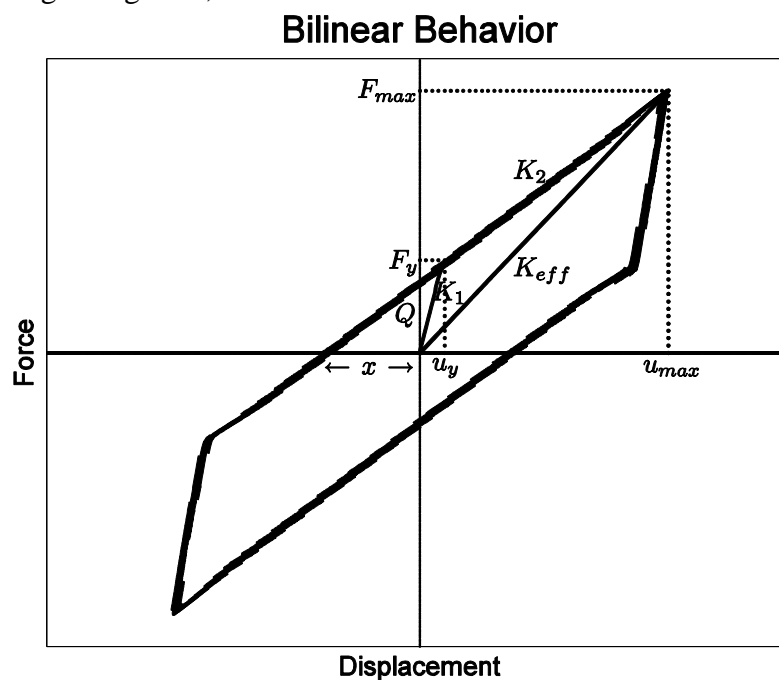


Figure 1. The hysteretic loop of the bilinear model.

$$\frac{F_{\max}}{F_y} = \frac{u_{\max} + x}{u_y + x} \quad (1)$$

with $x = Q/K_2$. Substitution of the expression of F_{\max} given by equation (1) to the definition of $K_{eff} = F_{\max}/u_{\max}$ gives

$$K_{eff} = K_1 \frac{u_y}{u_{\max}} \frac{\frac{u_{\max}}{u_y} + \frac{Q}{K_2 u_y}}{1 + \frac{Q}{K_2 u_y}} \quad (2)$$

in which the relation $F_y = K_1 u_y$ has been used. Introducing the definition of the traditional displacement ductility $\mu = u_{\max}/u_y$ and the second-to-the-first stiffness ratio $\alpha = K_2/K_1$, the expression given by (2) simplifies to

$$K_{eff} = K_1 \frac{1 + \alpha(\mu - 1)}{\mu} \quad (3)$$

and in terms of periods equation (3) gives

$$T_{eff} = T_1 \sqrt{\frac{\mu}{1 + \alpha(\mu - 1)}} \quad (4)$$

Equations (3) and (4) are well known in the literature (Hwang and Sheng [24], [25], Chopra and Goel [26], Miranda and Ruiz Garcia [10] and references reported therein). They are popular geometric relations which are valid for any value of the parameters K_1 , α and μ . Nevertheless, while the expression given by equation (4) is geometrically correct, its physical value remains feeble since there is no physical argument that associates the results of equation (4) with the vibration period of mass supported on a bilinear hysteretic system.

Figure 2 plots with a heavy solid line the values of the period shift, T_{eff}/T_1 , as given by equation (4) as a function of the displacement ductility μ for the widely used value of $\alpha = 0.05$ (Iwan and Gates [11]). The period shift, T_{eff}/T_1 , eventually tends asymptotically to the value $T_2/T_1 = 1/\sqrt{\alpha}$ as the value of the ductility μ increases. Nevertheless, with equation (4) this asymptotic value is approximated for values of ductility $\mu > 40$ (Makris and Kampas [27]).

With reference to the various methods assessed in this study it is worth noting that any proposed expression of the effective period, T_{eff} , which results from a physically sound procedure shall satisfy the constraint that the proposed period T_{eff} shall always be larger than the first period T_1 and less than or equal to the second period T_2 which corresponds to the second slope of the system. Accordingly,

$$1 < \frac{T_{eff}}{T_1} \leq \frac{T_2}{T_1} = \frac{1}{\sqrt{\alpha}} \quad (5)$$

$$\alpha = K_2/K_1 = 0.05 = 1/20$$

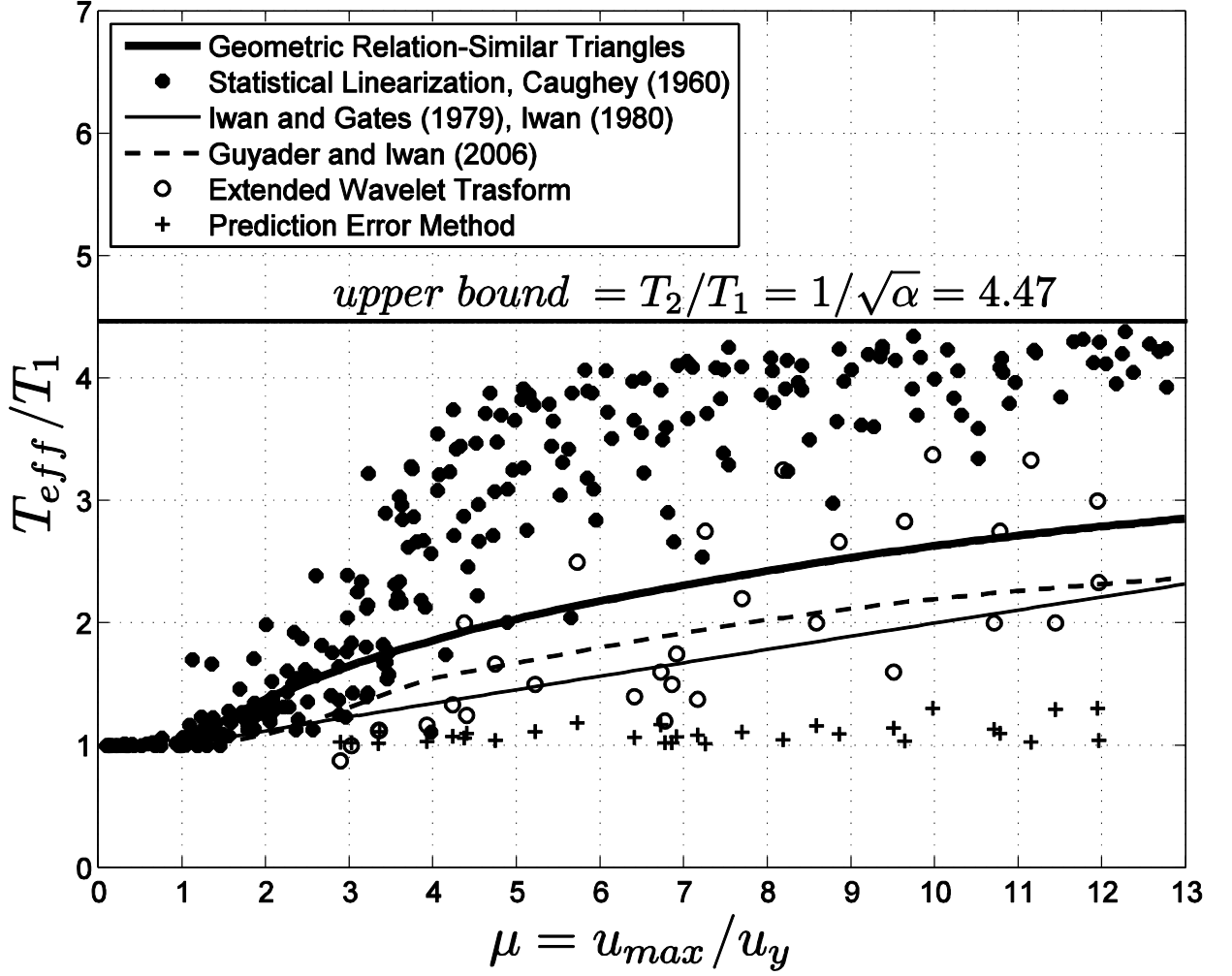


Figure 2. Values of the effective period, T_{eff} , as a function of the displacement ductility, $\mu = u_{max}/u_y$, as they result (a) from similar triangles, (b) equivalent linearization methods that minimize response differences and (c) signal processing methods that examine the response signal alone.

3. STOCHASTIC EQUIVALENT LINEARIZATION

Within the context of statistical linearization where a nonlinear system with a narrow-band response is subjected to a broadband excitation, we consider a one-degree-of-freedom system with bilinear behavior subjected to a stationary, zero-mean acceleration process $g(t)$, which does not necessarily have a white spectrum, expressed in the frequency domain by its power spectrum $G(\omega)$. The equation of motion of the bilinear system with mass m reads

$$\ddot{u}(t) + 2\xi\omega_1\dot{u}(t) + \frac{F(u,\dot{u})}{m} = -g(t), \text{ with } u(0), \dot{u}(0) = 0 \quad (6)$$

where $F(u,\dot{u})$ is the nonlinear restoring force,

$$F(u,\dot{u}) = \alpha K_1 u(t) + (1 - \alpha) K_1 u_y z(t), \quad (7)$$

in which K_1 is the first slope of the bilinear loop, u_y is the yield displacement shown in Figure 1, $\alpha = K_2 / K_1$ is the ratio of the postyield stiffness K_2 to the initial elastic stiffness K_1 , and $z(t)$ is the internal dimensionless parameter with $|z(t)| \leq 1$ that is governed by

$$u_y \dot{z}(t) + \gamma |\dot{u}(t)| |z(t)| |z(t)|^{n-1} + \beta \dot{u}(t) |z(t)|^n - \dot{u}(t) = 0. \quad (8)$$

The model given by equations (7) to (8) is the Bouc-Wen model (Wen [28], [29]) in which β , γ and n are dimensionless quantities that control the shape of the hysteretic loop. Defining $\omega_1^2 = K_1 / m$ equation (6) reduces to

$$\ddot{u}(t) + 2\xi\omega_1\dot{u}(t) + \omega_1^2 [\alpha u(t) + (1 - \alpha)u_y z(t)] = -g(t) \quad (9)$$

The quantity $\varphi(u, \dot{u}) = \alpha u(t) + (1 - \alpha)u_y z(t)$ appearing in equation (9) is a nonlinear function that governs the restoring force-deformation law.

The nonlinear response $u(t)$ appearing in equation (9) is approximated with the response $y(t)$ of an equivalent linear system with natural frequency ω_{eq} and viscous damping ratio ξ_{eq} given by the equation

$$\ddot{y}(t) + 2\xi_{eff}\omega_{eff}\dot{y}(t) + \omega_{eff}^2 y(t) = -g(t), \text{ with } y(0), \dot{y}(0) = 0 \quad (10)$$

According to the original and most widely used form of statistical linearization (Caughey [2], Roberts and Spanos [8], Giaralis and Spanos [14]) the parameters of the linear system given by equation (9) are defined by minimizing the expected value of the difference (error) between equations (9) and (10) in a least square sense with respect to the quantities ω_{eff} and ξ_{eff} . This criterion yields the following expressions for the effective (equivalent) linear parameters

$$\omega_{eff}^2 = \left(\frac{2\pi}{T_{eq}}\right)^2 = \frac{E\{u(t)\varphi(u, \dot{u})\}}{E\{u^2\}} \quad (11)$$

and

$$\xi_{eff} = \xi_1 \frac{\omega_1}{\omega_{eq}} + \frac{E\{\dot{u}(t)\varphi(u, \dot{u})\}}{E\{\dot{u}^2\}} \quad (12)$$

where $E\{\cdot\}$ denotes the expectation operator. In most cases (Caughey [2], Roberts and Spanos [8]) the unknown distribution of the response $u(t)$ of the nonlinear oscillator (bilinear system) is approximated for the purpose of evaluating the expected values by a zero-mean Gaussian process. Furthermore, it is also assumed that the variances of the process $u(t)$ and $y(t)$ are equal (Roberts and Spanos [8], Crandall [9]). This leads to

$$E\{u(t)^2\} = \int_0^\infty \frac{G(\omega)}{(\omega^2 - \omega_{eq}^2)^2 + (2\xi_{eq}\omega\omega_{eq})^2} d\omega \quad (13)$$

and

$$E\{\dot{u}(t)^2\} = \int_0^\infty \frac{\omega^2 G(\omega)}{(\omega^2 - \omega_{eq}^2)^2 + (2\xi_{eq}\omega\omega_{eq})^2} d\omega \quad (14)$$

where $G(\omega)$ is the power spectrum of the stationary, zero-mean acceleration process $g(t)$. Substitution of equations (13) and (14) into the equations (11) and (12) gives the

effective parameters of the equivalent linear system (Caughey [1], Roberts and Spanos [8], Giaralis and Spanos [14]).

$$\omega_{eff}^2 = \left(\frac{2\pi}{T_{eff}}\right)^2 = \omega_1^2 \left\{ 1 - \frac{8(1-\alpha)}{\pi} \int_1^\infty \left(\frac{1}{v^3} + \frac{1}{v\theta}\right) \sqrt{v-1} e^{-v^2/\theta} dv \right\} \quad (15)$$

and

$$\xi_{eff} = \xi_1 \frac{\omega_1}{\omega_{eff}} + \left(\frac{\omega_1}{\omega_{eff}}\right)^2 \frac{1-\alpha}{\sqrt{\pi\theta}} \operatorname{erfc}\left(\frac{1}{\sqrt{\theta}}\right) \quad (16)$$

where

$$\theta = 2 \frac{E\{u(t)^2\}}{u_y^2} = 2 \frac{\int_0^\infty \frac{G(\omega)}{(\omega^2 - \omega_{eff}^2)^2 + (2\xi_{eff}\omega\omega_{eff})^2} d\omega}{u_y^2} \quad (17)$$

In equation (15) the parameter $a = K_2 / K_1$, is introduced with equation (7). Figure 3 shows the graph of the integral

$$I(\theta) = \int_1^\infty \left(\frac{1}{v^3} + \frac{1}{v\theta}\right) \sqrt{v-1} e^{-v^2/\theta} dv \quad (18)$$

appearing in equation (15) is a function of the variable $\theta = 2E\{u(t)^2\}/u_y^2$. At this point it is worth investigating the limiting values of $I(\theta)$ as θ tends either to zero or infinity.

When $\theta \rightarrow 0$, the exponential term of the integrand suppresses any polynomial growth; and $I(\theta) = 0$. Accordingly from equation (15),

$$\lim_{\theta \rightarrow 0} \omega_{eff}^2 = \omega_1^2 \quad (19)$$

showing that when θ is small; the effective frequency ω_{eff} is essentially ω_1 ($T_{eff} = T_1$). On the other hand,

$$\lim_{\theta \rightarrow \infty} I(\theta) = \int_1^\infty \frac{\sqrt{v-1}}{v^3} dv = \frac{\pi}{8} \quad (20)$$

Substitution of the result from equation (19) into equation (14) gives

$$\lim_{\theta \rightarrow \infty} \omega_{eff}^2 = a\omega_1^2 = \omega_2^2 \quad (21)$$

showing that for large values of θ , the effective frequency is ω_2 ($T_{eff} = T_2 = T_1 / \sqrt{a}$). The limiting values offered by equations (19) and (21) show that the statistical linearization method of bilinear systems as initially developed by Caughey [1] satisfies the physical inequalities given by (5). With the two limiting values of equation (15) established, our analysis proceeds by computing the effective period, T_{eff} , as offered by equation (15) by subjecting the seven (7) bilinear systems listed in Table 1 to three white noise excitations generated by MATLAB [20]. The white spectrum used for the realizations in this study is an unnecessary strong requirement on the excitation $g(t)$ which merely needs to be a stationary, zero mean signal. An in depth study on the ‘‘admissible’’ power spectra that represent a Gaussian stationary process, $g(t)$, which at the same time are compatible in a stochastic sense with given design spectra has been presented recently by Giaralis and Spanos [14]. An alternative approach to identify the equivalent linear system of a bilinear hysteretic

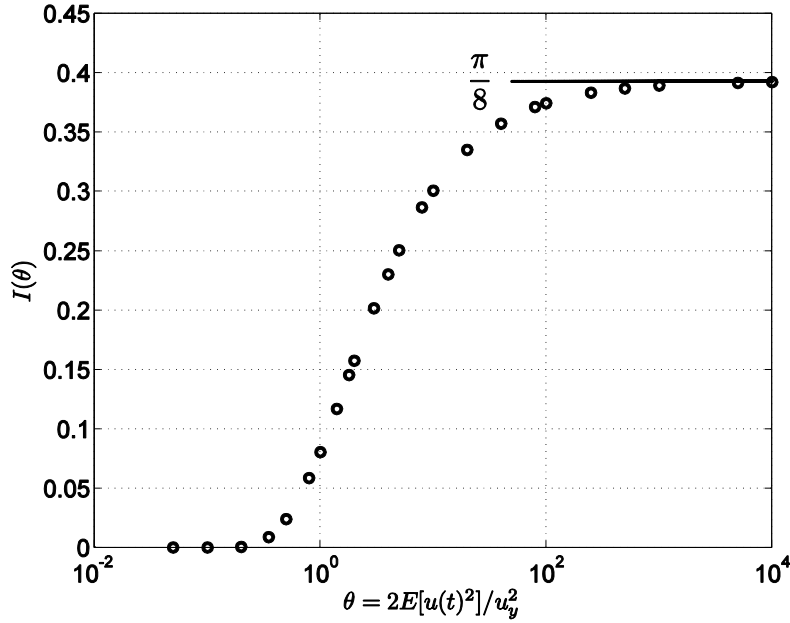


Figure 3. Graph of the integral $I(\theta)$ appearing in equation (15).

system has been presented by Politopoulos and Feau [30] and references reported therein.

Herein, we merely use white spectra in an effort to uncover the challenges associated with the exercise to compute/identify the “effective period” of a bilinear system. Each of the three MATLAB realizations was used to excite all 7 bilinear systems listed in Table 1 and the levels of ductilities achieved were recorded. Subsequently, each excitation was gradually amplified so that each bilinear system achieved various levels of ductilities up to the value of $\mu = 12$. The bilinear systems listed in Table 1 have, $a = 0.05$, and were selected so that their parameters (T_1, u_y and Q) correspond to typical values of reinforced concrete and steel structures (see Table 1).

The response of the bilinear system is computed by solving equation (9) together with equation (8). From the nonlinear response analysis the peak deformation u_{\max} , was retained to compute the ductility demand of the response $\mu = u_{\max} / u_y$.

The values of T_{eff} of all seven bilinear systems listed in Table 1 as they result from statistical linearization via equation (15) are shown in Figure 2 with heavy dark dots for various values of ductility levels. The majority of these dots lie well above the

Table I. Parameters of bilinear systems examined in this study with $a = 0.05$

Model	$T_1(s)$	$T_2(s)$	$u_y(m)$	$Q/m(g)$
1	0.3	1.34	0.0050	0.212
2	0.4	1.79	0.0100	0.239
3	0.45	2.00	0.0026	0.05
4	0.5	2.24	0.0100	0.153
5	0.6	2.68	0.0200	0.212
6	0.67	3.00	0.0059	0.05
7	0.89	4.00	0.0104	0.05

heavy dark line –that is the geometric relation given by equation (4) and they tend to accumulate close to the upper bound value $T_2 = T_1 / \sqrt{a}$. The differences between the predictions of the effective period, T_{eff} , between equations (4) and (15) is anywhere between 50% and 100%.

4. THE WORK OF IWAN AND GATES [11], IWAN [12] AND GUYADER AND IWAN [13]

Early theoretical work of the effective period and damping of stiffness-degrading structures was presented by Iwan and Gates [11]. The hysteretic model examined by Iwan and Gates [11] is a collection of linear elastic and Coulomb slip elements which can approximate the phenomenon of cracking, yielding and crushing. A special case of their hysteretic model is the bilinear model that is of interest in this study. Their study was motivated by the yielding response of traditional concrete and steel structures where the initial elastic stiffness, K_1 , is a dominant parameter of the model; while, the displacement ductility assumes single digit values (say $\mu \leq 8$). Iwan and Gates [11] observed that the average inelastic response spectra resemble the linear response spectra except for a translation along an axis of constant spectral displacement. The above observation was a major contribution at that time for it indicates that the effective period of each corresponding linear system would be of some constant multiple of the first period of the hysteretic system.

$$T_{eff} = CT_1 \quad (22)$$

Equation (22) is similar to equation (4); however, in the work of Iwan and Gates [11] the constant, C , appearing in equation (22) is not an outcome from similar triangles (which result by assuming that K_{eff} is the slope of the line that connects the axis origin with the point on the backbone curve where we anticipate the maximum displacement to occur), but is the outcome from minimizing the root mean square (RMS) of the error between the average earthquake spectral displacements of a bilinear system and a family of potentially equivalent linear systems. Table 2 compares the values of C appearing in equation (22) for the bilinear system with $\alpha = K_2 / K_1 = 0.05$ as computed by Iwan and Gates [11] together with the corresponding values of the term $\sqrt{\mu/(1 + \alpha(\mu - 1))}$ appearing in equation (4).

Table II indicates that for moderate values of ductility, the period shift (T_{eff} / T_1) as predicted by equation (4) is appreciably longer (i.e. 42% longer for $\mu = 4.0$) than the Table II. Comparison of the Geometric Relation between T_{eff} and T_1 and the Results presented by Iwan and Gates [11] and Iwan [12].

$\mu = \frac{u_{max}}{u_y}$	$\sqrt{\mu/(1 + \alpha(\mu - 1))}$ $\alpha = 0.05$	$C = T_{eff} / T_1$ Iwan and Gates [11]	Eq.(17) Iwan [12]
0.6	-	1.000	-
1.0	1.000	1.000	1.000
1.5	1.210	1.000	1.063
2.0	1.380	1.130	1.121
4.0	1.865	1.317	1.339
8.0	2.434	1.573	1.752

period shift computed by Iwan and Gates [11] after minimizing the RMS of the difference between the equivalent elastic and inelastic average earthquake spectra. Consequently, for moderate values of ductility ($2.0 \leq \mu \leq 8.0$) the findings of Iwan and Gates [11] depart appreciably to the lower side from the results of the geometric relation given by equation (4).

In a subsequent publication (Iwan [12]), the period shift, T_{eff}/T_1 , presented in Table II was graphed as a function of the ductility, $\mu = u_{max}/u_y$. The least square log-log fit of these data resulted for a bilinear system with, $\alpha = K_2/K_1 = 0.05$, the following expression

$$T_{eff} = [1 + 0.121(\mu - 1)^{0.939}]T_1, \quad \mu \leq 8 \quad (23)$$

Figure 2 plots with a thin solid line the values of the period shift, T_{eff}/T_1 , as offered by equation (23) for $\alpha = 0.05$ and up to values of ductility, $\mu = 12$. These values are compared with the results from the geometric relation given by equation (4) and the results from the statistical linearization formulation (dark dots) as they offered by equation (15). What is striking about this comparison is that the differences between equation (23) presented by Iwan [12] and equation (15) presented by Caughey [1] are anywhere between 100% and 150%. Given that both methodologies are sound and that their mathematical foundations are correct, the comparison of the values for the effective period of bilinear systems offered in Figure 2 indicates that T_{eff} is a quantity that has an elusive physical meaning, it depends strongly on the methodology adopted to calculate it and shall be used with caution and only within the limitations of the specific application.

At this point it is worth reiterating that the statistical linearization method as formulated by Caughey [1] and documented by Roberts and Spanos [8]: (a) uses as ground excitation a stationary, zero-mean acceleration process; and (b) the value of T_{eff} result after minimizing the expected value of the difference (error) between the displacement response time histories of the linear and nonlinear systems. On the other hand, the method presented by Iwan and Gates [11] which leads to equation (23) (Iwan [12]): (a) uses as ground excitation historic earthquake records; and (b) the values of T_{eff} result after minimizing the overall RMS error between the average spectral displacements of a bilinear system and a family of potentially equivalent linear systems.

In view of these striking differences between the values of the estimated T_{eff} our study proceeds with the estimation of the effective period, T_{eff} , by trying to identify a dominant vibration period in the response of the bilinear system by using mathematical formal and objective techniques.

Some 35 years later Guyader and Iwan [13] revisited the problem of estimating equivalent linear parameters of nonlinear systems after introducing a measure on “engineering acceptability” –that is conservative displacement predictions are more acceptable than unconservative predictions. Building on the earlier work of Iwan and Gates [11] and Iwan [12], Guyader and Iwan [13] presented the following set of expressions for the period shift in a bilinear system

$$T_{eff} = [1 + 0.1145(\mu - 1)^2 - 0.0178(\mu - 1)^3]T_1, \quad \text{for } \mu < 4.0 \quad (24a)$$

$$T_{eff} = [1 + 0.1777 + 0.1240(\mu - 1)]T_1, \quad \text{for } 4.0 \leq \mu \leq 6.5 \quad (24b)$$

$$T_{eff} = [1 + 0.768(\sqrt{\frac{\mu-1}{1+0.05(\mu-2)}} - 1)]T_1, \text{ for } \mu > 6.5 \quad (24c)$$

Figure 2 plots with a dashed line the values of the period shift T_{eff}/T_1 offered by equations (24 a,b,c) for $a = 0.05$ up to values of ductility $\mu = 12$. These values are above the initial values proposed by Iwan and Gates [11], Iwan [12] given by equations (23); yet, they remain below the over conservative values offered by the geometric relation given by equation (4).

5. THE WORK OF GIARALIS AND SPANOS [14]

An effort to bridge the gap between the power spectrum appearing in stochastic equivalent linearization (see equations (15) to (17)) and a design (earthquake) acceleration spectrum, $S_a(\omega_{eff}, \xi)$, was recently presented by Giaralis and Spanos [14]. In their study, the core equation for relating S_a to a one-sided power spectrum, $G(\omega)$ representing a Gaussian stationary process $g(t)$ assumes the expression

$$S_a(\omega_{eff}, \xi) = \eta_{eff,G} \omega_{eff}^2 \sqrt{E\{u(t)^2\}} = \eta_{eff,G} \omega_{eff}^2 \left[\int_0^\infty \frac{G(\omega)}{(\omega^2 - \omega_{eff}^2)^2 + (2\xi\omega\omega_{eff})} d\omega \right] \quad (25)$$

in which the correction factor $\eta_{eff,G}$ (coined as the “peak” factor in the original paper, Giaralis and Spanos [14]) establishes the equivalence, with probability of exceedence p , between the earthquake acceleration spectrum, S_a and $G(\omega)$ (Vanmarcke [25]). The exact determination of $\eta_{eff,G}$ is associated with the first passage problem for which a closed form solution is not available. In order to address this challenge, Giaralis and Spanos [14] adopted a semi-empirical formula known to be reasonably reliable for earthquake engineering applications (Vanmarcke [31], Der Kiureghian [32]); while assuming that the aforementioned probability of exceedence is $p = 0.5$. The elaborated methodology presented by Giaralis and Spanos [14] eventually involves a recursive procedure to evaluate $G(\omega)$ and its implementation is beyond the scope of this study.

6. WAVELET ANALYSIS

In the above-reviewed equivalent linearization techniques (Caughey [1], Iwan and Gates [11], Guyader and Iwan [13] and Giaralis and Spanos [14]) the effective period of the bilinear system is estimated by engaging a linear system. The wavelet analysis, presented in this section, examines the response signal alone without minimizing any difference with the response of an equivalent linear oscillator.

Over the last two decades, wavelet transform analysis has emerged as a unique new time-frequency decomposition tool for signal processing and data analysis. There is a wide literature available regarding its mathematical foundation and its applications (Mallat [16], Addison [17], Newland [18] and references reported therein). Wavelets are simple wavelike functions localized on the time axis. For instance, the second derivative of the Gaussian distribution, $e^{-t^2/2}$, known in seismology literature as the symmetric Ricker wavelet (Ricker [33], [34] and widely referred as the “Mexican Hat” wavelet, Addison [17]),

$$\psi(t) = (1 - t^2)e^{-t^2/2} \quad (26)$$

is a widely used wavelet. Similarly the time derivative of equation (25) or a one cycle cosine function are also wavelets. A comparison on the performance of various

symmetric and antisymmetric wavelet to fit acceleration records is offered in Vassiliou and Makris [35]. In order for a wavelike function to be classified as a wavelet, the wavelike function must have: (a) finite energy,

$$E = \int_{-\infty}^{+\infty} |\psi(t)|^2 dt < \infty \quad (27)$$

and (b) a zero mean. In this work we are merely interested to achieve a local matching of the response history of a bilinear system with a wavelet that will offer the best estimates of period, T_l . Accordingly, we perform a series of inner products (convolutions) of the acceleration response history of the bilinear system, $\ddot{u}(t)$ with the wavelet $\psi(t)$ by manipulating the wavelet through a process of translation (i.e. movement along the time axis) and a process of dilation-contraction (i.e. spreading out or squeezing of the wavelet)

$$C(s, \xi) = w(s) \int_{-\infty}^{+\infty} \ddot{u}(t) \psi\left(\frac{t-\xi}{s}\right) dt \quad (28)$$

The values of $s = S$ and $\xi = \Xi$, for which the coefficient, $C(s, \xi) = C(S, \Xi)$ becomes maximum offer the scale and location of the wavelet $w(s) \psi\left(\frac{t-\xi}{s}\right)$ that locally best matches the acceleration record, $\ddot{u}(t)$. Equation (28) is the definition of the wavelet transform. The quantity $w(s)$ outside the integral in equation (28) is a weighting function. Typically $w(s)$ is set equal to $1/\sqrt{s}$ in order to ensure that all wavelets $\psi_{s,\xi}(t) = w(s) \psi\left(\frac{t-\xi}{s}\right)$ at every scale s have the same energy, and according to equation (27)

$$\int_{-\infty}^{\infty} |\psi_{s,\xi}(t)|^2 dt = \int_{-\infty}^{\infty} \left| \frac{1}{\sqrt{s}} \psi\left(\frac{t-\xi}{s}\right) \right|^2 dt = \|\psi_{s,\xi}(t)\|_2 = \text{constant}, \quad \forall s \quad (29)$$

The same energy requirement among all the daughter wavelets $\psi_{s,\xi}(t)$ is the default setting in the MATLAB wavelet toolbox and has been used by Baker [36]; however, the same energy requirement is, by all means, not a restriction. Clearly there are applications where it is more appropriate that all daughter wavelets $\psi_{s,\xi}(t)$ at every scale s to enclose the same area ($w(s) = 1/s$) or have the same maximum value ($w(s) = 1$). However, in this paper there is no particular need for not using the default same energy requirement for the daughter wavelets.

The multiplication factor

$$\lambda(S, \Xi) = \frac{C(S, \Xi)}{w^2(s) \cdot S \cdot E} \quad (30)$$

where E is the energy of the mother wavelet, is needed in order for the best matching wavelet, $\psi_{s,\Xi}(t) = w(s) \psi\left(\frac{t-\Xi}{S}\right)$, to assume locally the amplitude of the acceleration record.

One of the challenges with any given wavelet is that upon is selected as the interrogating signal there is a commitment on the phase and the number of cycles of the mother wavelet. This challenge has been recently addressed by Vassiliou and Makris [35] who proposed the extended wavelet transform where in addition to a time translation and a dilation-contraction, the proposed transform allows for a phase modulation and the addition of half cycles.

In the classical wavelet transform defined with equation (28) the mother wavelet is only subjected to a translation together with a dilation-contraction, $\psi\left(\frac{t-\xi}{s}\right)$. The

dilation contraction is controlled with the scale parameter s ; while, the movement of the wavelet along the time axis is controlled with the translation time, ξ . For instance, any daughter wavelet of the symmetric Ricker mother wavelet given by equation (26) assumes the form

$$\psi\left(\frac{t-\xi}{s}\right) = \left[1 - \left(\frac{t-\xi}{s}\right)^2\right] e^{-\frac{1}{2}\left(\frac{t-\xi}{s}\right)^2} \quad (31)$$

In equation (31) the relation between the scale of the wavelet s and the period of the pulse, $T_p = 1/f_p$ is $s = T_p \sqrt{2}/2\pi$ (Addison [17]). The need to include four parameters in a mathematical expression of a simple wavelike function has been presented and addressed by Mavroeidis and Papageorgiou [37]. They identified as the most appropriate analytical expression the Gabor [38] “elementary signal” which they slightly modified to facilitate derivations of closed-form expressions of the spectral characteristics of the signal and response spectra. The Gabor [38] “elementary signal” is defined as

$$g(t) = e^{-\left(\frac{2\pi f_p}{\gamma}\right)^2 t^2} \cos\left[2\pi f_p t + \varphi\right] \quad (32)$$

which is merely the product of a harmonic oscillation with a Gaussian envelop. In equation (32), f_p is the frequency of the harmonic oscillation, φ is the phase angle and γ is a parameter that controls the oscillations characters of the signal. The Gabor wavelike signal given by equation (32) does not have a zero mean; therefore, it cannot be a wavelet within the context of the wavelet transformation.

Nevertheless, the elementary signal proposed by Mavroeidis and Papageorgiou [37] to approximate velocity pulses is a slight modification of the Gabor signal given by equation (32) where the Gaussian envelope has been replaced by an elevated cosine function.

$$v(t) = \frac{1}{2} \left(1 + \cos\left(\frac{2\pi f_p}{\gamma} t\right)\right) \cos(2\pi f_p t + \varphi) \quad (33)$$

Clearly the wavelike signal given by equation (33) does not always have a zero mean; therefore it cannot be a wavelet within the context of wavelet transform. Nevertheless, the time derivative of the elementary velocity signal given by equation (33)

$$\frac{dv(t)}{dt} = \frac{\pi f_p}{\gamma} \left(\sin\left(\frac{2\pi f_p}{\gamma} t\right) \cos(2\pi f_p t + \varphi) + \gamma \sin(2\pi f_p t + \varphi) \left(1 + \cos\left(\frac{2\pi f_p}{\gamma} t\right)\right) \right) \quad (34)$$

is by construction a zero-mean signal and is defined in this paper as the Mavroeidis and Papageorgiou (M&P) wavelet. After replacing the oscillatory frequency, f_p , with the inverse of the scale parameter the M&P wavelet is defined as

$$\psi\left(\frac{t-\xi}{s}, \gamma, \varphi\right) = \left(\sin\left(\frac{2\pi}{s\gamma}(t-\xi)\right) \cos\left(\frac{2\pi}{s}(t-\xi) + \varphi\right) + \gamma \sin\left(\frac{2\pi}{s}(t-\xi) + \varphi\right) \right) \left(1 + \cos\left(\frac{2\pi}{\gamma s}(t-\xi)\right) \right) \quad (35)$$

The novel attraction in the M&P wavelet given by equation (35) is that in addition to the dilation-contraction and translation $\left(\frac{t-\xi}{s}\right)$, the wavelet can be further manipulated by modulating the phase, φ , and the parameter γ , which controls the oscillatory character (number of half cycles). We can now define the four parameter wavelet transform as

$$C(s, \xi, \gamma, \varphi) = w(s, \gamma, \varphi) \int_{-\infty}^{+\infty} \ddot{u}(t) \psi\left(\frac{t-\xi}{s}, \gamma, \varphi\right) dt \quad (36)$$

The inner product given by equation (36) is performed repeatedly by scanning not only all times, ξ , and scales, s , but also by scanning various phases, $\varphi = \{0, \pi/4, \pi/2, 3\pi/4\}$, and various values of oscillatory character of the signal $\gamma = \{1.0, 1.5, 2.0, 2.5, 3.0\}$. When needed more values of φ and γ may be scanned. The quantity $w(s, \gamma, \varphi)$ outside the integral is a weighting function which is adjusted according to the application. For instance, when all daughter wavelets have the same area the wavelet transform emphasizes on the shorter period pulses; whereas when all daughter wavelets have the same amplitude the wavelet transform emphasizes on the longer period pulses (Vassiliou and Makris [35]).

Figure 4 (top-left) plots with a heavy dark line the best matching Mavroeidis and Papageorgiou (M&P) wavelet (Vassiliou and Makris [35]) on the acceleration response history of a bilinear system with strength $Q/m = 0.153g$, first period $T_1 = 0.5s$ and $u_y = 0.01m = 1cm$ when subjected to the OTE ground motion recorded during the 1995 Aigion earthquake. The displacement ductility reached is $\mu = u_{max}/u_y = 6.76$ and the period of the best matching wavelet –that is the dominant vibration period is $T_{eff} = 1.20s$. Figure 5 (left) plots the 5% elastic displacement response spectrum of the OTE ground motion -1995 Aigion earthquake and for the period $T_{eff} = 1.20s$ as extracted with the wavelet analysis, the elastic spectral displacement is $S_D = 0.06m$. Note that the dominant pulse extracted with wavelet analysis depends on the weighting function, $w(s, \gamma, \varphi)$ appearing in front of the integral given by equation (36) (Vassiliou and Makris [35]). In this analysis $w(s, \gamma, \varphi)$ is selected in such a way so that all daughter wavelets in the analysis have the same energy. Next to this spectral value that corresponds to a displacement ductility of the inelastic system, $\mu = 6.76$, the period values (and the corresponding spectral displacement) offered by equations (23) ($T_{I\&G} = 0.81s$) and (24) ($T_{G\&I} = 0.94s$) and the geometric relation given by equation (4) ($T_{ST} = 1.15s$) are shown. Note that in this example the vibration period extracted with the wavelet analysis is longer than the period predicted with the minimization proposed by Iwan

and Gates [11] which is always shorter than the period which one computes with similar triangles (equation (4)). The spectral displacement that correspond to the vibration period extracted with the wavelet analysis ($T_{WA} = 1.20s$) is $SD = 0.06m$;

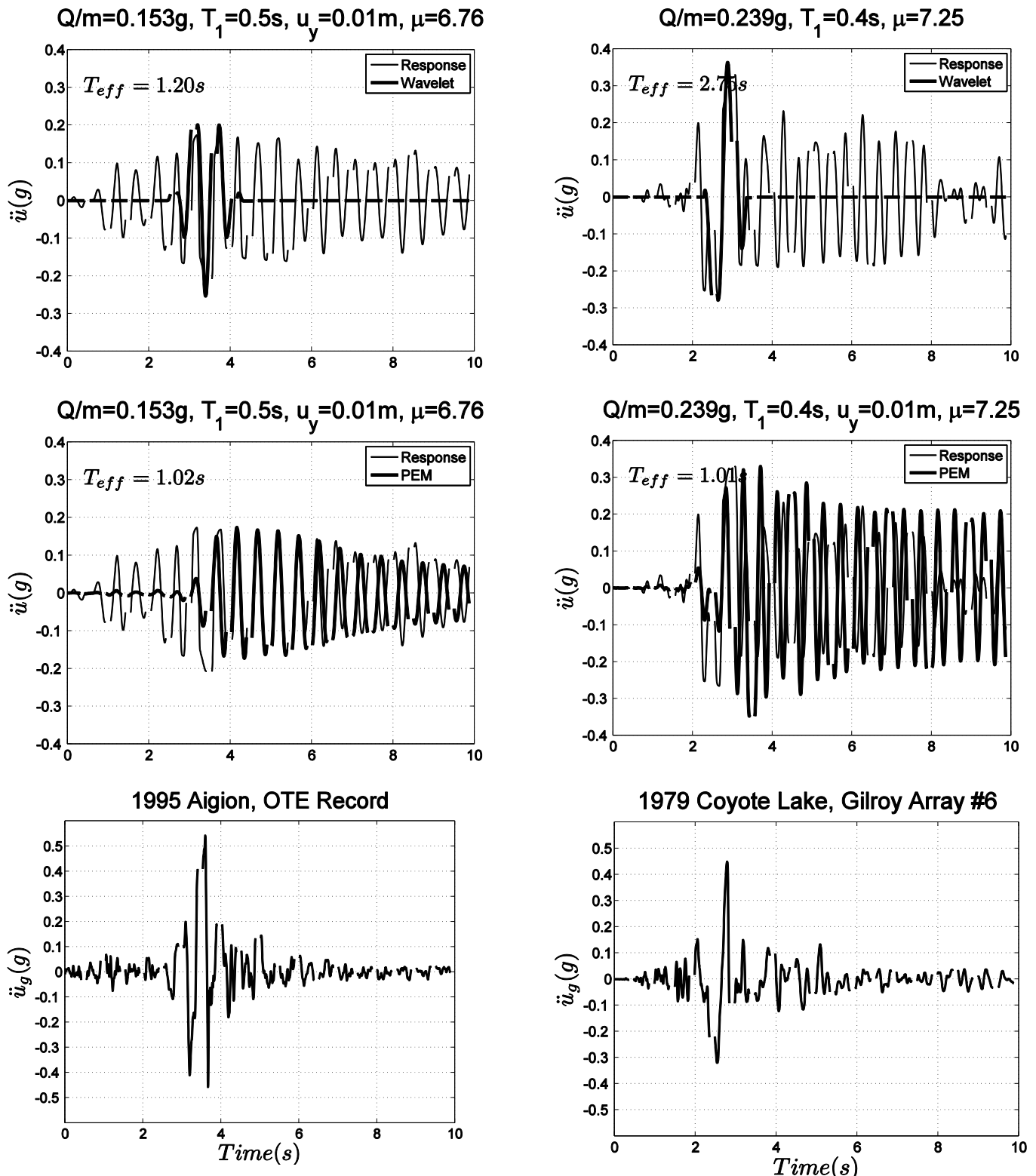


Figure 4. Matching the acceleration response histories of bilinear systems with wavelet analysis (top) and the Prediction Error Method (center) when they are subjected to records from the 1995 Aigion, Greece and the 1979 Coyote Lake earthquakes.

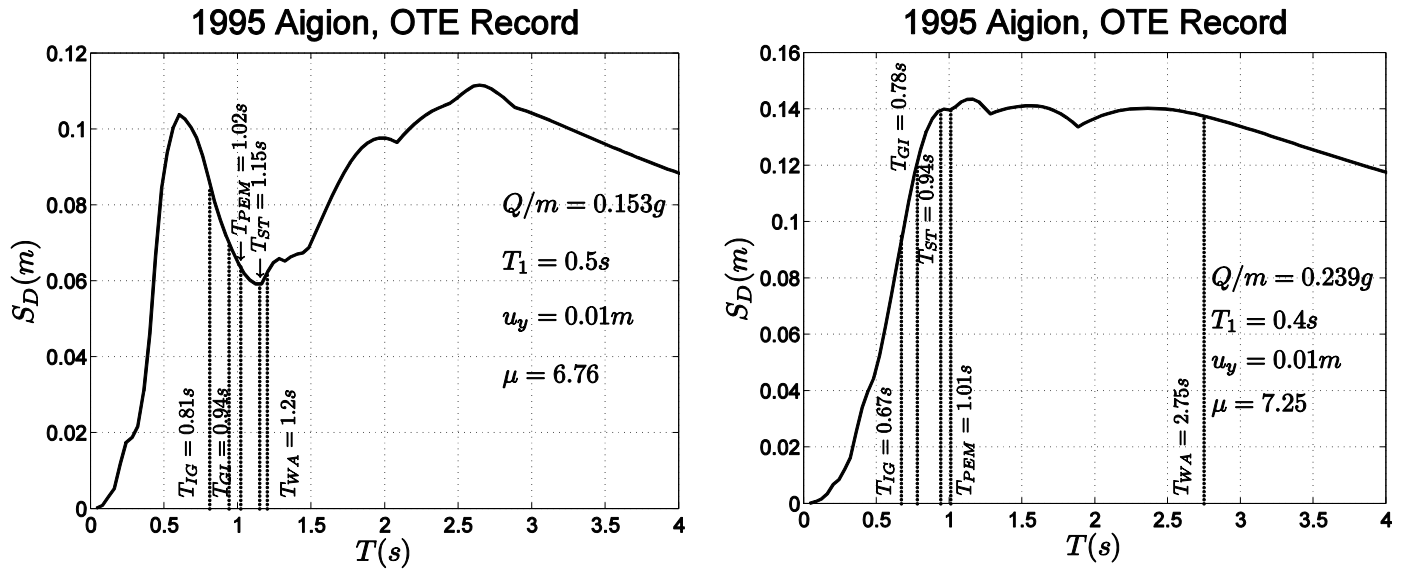


Figure 5. Elastic displacement response spectra of the two earthquake records shown in Figure 4(bottom) together with the effective period values of two bilinear systems as they result from the methods assessed in this study.

while $SD = 0.08m$ and more than $0.10m$ when equations (18) and (4) are used respectively.

Figure 4 (top-right) plots with a heavy dark line the best matching M&P wavelet (Vassiliou and Makris [35]) on the acceleration response history of a bilinear system with strength $Q/m = 0.239$, first period $T_1 = 0.4s$ and $u_y = 0.01m$ when subjected to Gilroy Array #6 ground motion recorded during the 1979 Coyote Lake earthquake. The displacement ductility reached is $\mu = u_{max} / u_y = 7.25$ and the period of the best matching wavelet –that is the dominant vibration period is $T_{eff} = 2.75s$.

Figure 5 (right) plots the 5% elastic displacement response spectrum of the Gilroy Array #6 ground motion -1995 Coyote Lake earthquake. For the period $T_{eff} = 2.75s$ as extracted with the wavelet analysis the spectral displacement is $SD = 0.014m$. Next to this spectral value that corresponds to a displacement ductility of the inelastic system, $\mu = 7.25$, the period values offered by equations (23) ($T_{I\&G} = 0.67s$) and (24) ($T_{G\&I} = 0.94s$) and the geometric relation given by equation (4) ($T_{ST} = 0.94s$) are shown.

Table III. Earthquake records selected as input motions in this study.

Earthquake	Record Station	Magnitude, M_w	PGA(g)
1966 Parkfield	CO2 (St. 065)	6.0	0.48
1979 Coyote Lake, CA	Gilroy Array #6 230	5.7	0.43
1983 Coalinga	Oil City 270	5.8	0.87
1983 Coalinga	Transmitter Hill 360	5.8	1.08
1983 Coalinga	Transmitter Hill 270	5.8	0.84
1986 North Palm Springs	North Palm Springs	6.1	0.69
1995 Aigion	OTE Building	6.2	0.54

The vibration periods extracted with wavelet analysis from the response of all bilinear systems listed in Table II when subjected to the historic records listed in Table III are also shown in Figure 2 with empty circles. These values are scattered, nevertheless,

most of them lie above the line defined by equation (18) (Iwan and Gates [11], Iwan [12]).

7. TIME DOMAIN ANALYSIS

Over the years, various powerful time domain methods have been developed and applied successfully. Perhaps, the most well known and powerful method in the system identification community is the Prediction Error Method (PEM).

It initially emerged from the maximum likelihood framework of Aström and Bohlin [19] and subsequently was widely accepted via the corresponding MATLAB [20] identification toolbox developed following the theory advanced by Ljung [21], [22], [23].

Figure 4(center-left) plots with a heavy dark line the signal generated with the prediction error method (PEM) that best identifies the acceleration response history of bilinear system with strength $Q/m = 0.155g$, first period $T_1 = 0.5s$ and $u_y = 0.01m = 1cm$ when subjected to the OTE ground motion recorded during the 1995 Aigion earthquake. The period of the best matching signal offered by PEM is $T_{eff} = 1.02s$. While the wavelet analysis (see Figure 4 top-left) concentrates on matching locally the most energetic pulse of the response history the prediction error method attempts to match to the extent possible a maximum segment of the response history. Consequently, the effective vibration period extracted with PEM will be in principle shorter than the periods extracted with wavelet analysis. Figure 4 (center-right) plots with a heavy dark line the signal generated with PEM that best identifies the acceleration response history of a bilinear system with strength $Q/m = 0.239g$, first period, $T_1 = 0.4s$ and $u_y = 0.01m$ when subjected to the Gilroy Array #6 ground motion recorded during the 1979 Coyote Lake earthquake. In this case the period of the best matching identification signal offered by PEM is $T_{eff} = 1.01s$; whereas the period of the best matching wavelet (see Figure 4 center left) is $T_{eff} = 2.75s$. The shape of the Gilroy Array #6 spectrum shown in Figure 5(right) is such that these two period values which are $2.75 - 1.01 = 1.74s$ apart correspond to comparable spectral displacements.

The vibration periods extracted with the prediction error method from the response of all bilinear systems listed in Table II are also shown in Figure 2 with crosses. These values are systematically close to the value of the first period, T_1 , of the bilinear system, indicating that the PEM tends to extract essentially the elastic period that manifest itself during the small-amplitude vibrations. The poor performance of the PEM in identifying the equivalent linear modal properties of 2-DOF systems with bilinear isolators has also been reported by Kampas and Makris [33].

8. CONCLUSIONS

This paper revisits and compares estimations of the effective period of bilinear systems exhibiting low to moderate ductility values as they result from: (a) Simple geometric relations associated with the bilinear loop, (b) stochastic equivalent linearization where the excitation process has a white spectrum, (c) the equivalent linearization method which minimize the difference between earthquake spectra presented by Iwan and Gates [11] and Guyader and Iwan [13], (d) best matching the most energetic pulse of the nonlinear response history with a four-parameter wavelet and (e) a time-domain method known as the Prediction Error Method (PEM).

The general conclusion is that the resulting values of the “effective period” (vibration period of the equivalent linear system) are widely scattered and they lie anywhere between the period values that correspond the first and the second slope of the bilinear system.

At any given ductility value, $\mu = u_{\max} / u_y$, the simple geometric relation, $T_{\text{eff}} = T_1 \sqrt{\mu / [1 + a(\mu - 1)]}$ appears to give the average value of T_{eff} among the scattered values offered by the aforementioned methods as summarized in Figure 2.

The stochastic equivalent linearization method in which the excitation process has a white spectrum yields effective period values which are systematically larger than the period values offered by the simple geometric relation, $T_{\text{eff}} = T_1 \sqrt{\mu / [1 + a(\mu - 1)]}$; while, the equivalent linearization method which minimizes the difference between the earthquake spectra (Iwan and Gates [11]) yields effective period values which are appreciable shorter. The revised expressions of Guyader and Iwan [13] which accounted for a conservative estimation of the effective period yield effective period values longer than the initial estimates of Iwan and Gates [12]; yet, shorter than the simple geometric relation.

In addition to methods (b) and (c), the study examined the performance of two signal processing methods that process the response history alone without minimizing any difference with the response of a potentially equivalent linear oscillator.

The best matching of the most energetic pulse of the nonlinear response history with a four-parameter wavelet transform yields vibration (“effective”) period values which are widely scattered confirming the main finding of this study that the concept of the “effective period” of a bilinear system has limited technical value and the results depend strongly on the methodology used.

Finally, the study show that the prediction error method attempts to match to the extent possible, a maximum segment of the nonlinear response history; therefore, concentrating on the small amplitude part of the nonlinear response; while, missing the local longer-period pulses which develop when the bilinear system experiences its larger ductility values.

ACKNOWLEDGEMENTS

This research has been co-financed by the European Union (European Social Fund – ESF) and Greek national funds through the Operational Program "Education and Lifelong Learning" of the National Strategic Reference Framework (NSRF) - Research Funding Program: Heracleitus II. Investing in knowledge society through the European Social Fund.

REFERENCES

1. Caughey, T.K. Random excitation of a system with bilinear hysteresis. *Journal of Applied Mechanics* 1960; 27,649-652.
2. Caughey, T.K. Equivalent linearization techniques. *Journal of Acoustical Society of America* 1963; 35,1706-1711.
3. Chopra A. Elastic response spectrum: A historical note. *Journal of Earthquake Engineering and Structural Dynamics* 2007; 36, 3-12.
4. Veletsos A.S., and Newmark, N.M. Effect of inelastic behavior on the response of simple systems to earthquake motions. In: *Proceedings of the second world conference on earthquake engineering, Japan 1960*; 2,895-912.

5. Veletsos A.S., Newmark N.M., Chelepati C.V. Deformation spectra for elastic and elastoplastic systems subjected to ground shock and earthquake motions. Proceedings of the 3rd World Conference on Earthquake Engineering, vol. II, Wellington, New Zealand 1969, 663-682.
6. Veletsos A.S., Vann W.P. Response of ground-excited elastoplastic systems. Journal of Structural Division (ASCE) 1971; 97(ST4),1257-1281.
7. Rosenblueth E, Herrera I. On a kind of hysteretic damping. Journal of Engineering Mechanics Division ASCE, 1964; 90:37– 48.
8. Roberts J.B and Spanos P.D. Random vibration and statistical Linearization. New York: Dover Publications, 1990.
9. Crandall, S.H. A half-century of stochastic equivalent linearization. Journal of Structural Control and Health Monitoring 2006; 13:27-40.
10. Miranda, E., and Ruiz-Garcia, J. Evaluation of approximate methods to estimate maximum inelastic displacement demands. Journal of Earthquake Engineering and Structural Dynamics, 2002; 31, 539-560.
11. Iwan W.D., and Gates N.C. The effective period and damping of a class of hysteretic structures. Journal of Earthquake Engineering and Structural Dynamics 1979; 7,199-211.
12. Iwan W.D. Estimating inelastic response spectra from response spectra. Journal of Earthquake Engineering and Structural Dynamics 1980, 8,375-388.
13. Guyader, A., C., and Iwan, W., D. Determining Equivalent Linear Parameters for Use in a Capacity Spectrum Method of Analysis. Journal of Structural Engineering, 2006; 132, 59-67.
14. Giaralis A., and Spanos P.D. Effective linear damping and stiffness coefficients of nonlinear systems for design spectrum base analysis, Journal of Soil Dynamics and Earthquake Engineering 2010; 30, 798-810.
15. Grossman, A. and Morlet, J. Decomposition of Hardy functions into square integrable wavelets of constant shape, SIAM J. Math. Anal. 1984; 15(4):723-736.
16. Mallat S. G. A wavelet tour of signal processing. Academic Press, 1999.
17. Addison P. S. The illustrated wavelet transform handbook. Institute of Physics Handbook, 2002.
18. Newland, D.E. An Introduction to Random Vibrations, Spectral and Wavelet Analysis, Third Edition, Longman Singapore Publishers, 1993.
19. Aström, K. J., and Bohlin T. Numerical identification of linear dynamic systems from normal operating records. IFAC Symposium on Self-Adaptive Systems, Teddington, England, 1965.
20. MATLAB. High-performance Language Software for Technical Computation. The MathWorks, Inc: Natick, MA, 2002.
21. Ljung L. System Identification-Theory for the User, Prentice-Hall, New Jersey, 1987.
22. Ljung L. State of the Art in Linear System Identification: Time and Frequency Domain Methods. Proceedings of '04 American Control Conference 1994; 1,650-660.
23. Ljung L. Prediction Error Estimation Methods. Circuits Systems Signal Processing 2002; 21: 11-21.
24. Hwang, J.S., and Sheng L.H. Equivalent elastic seismic analysis of base-isolated bridges with lead-rubber bearings. Journal of Engineering Structures, 1993; 16(3),201-209.

25. Hwang, J.S., and Sheng L.H. Effective stiffness and Equivalent Damping of Base-Isolated Bridges. *Journal of Structural Engineering*, 1994; 119(10), 3094-3101.
26. Chopra, A., and Goel, R., K. Evaluation of NSP to Estimate Seismic Deformation: SDF Systems. *Journal of Structural Engineering*, 2000; 126(4), 482-490.
27. Makris N., and Kambas G. The Engineering Merit of the “Effective Period” of Bilinear Isolation Systems, *Earthquakes and Structures*, in press.
28. Wen Y., K. Approximate method for nonlinear random vibration. *Journal of Engineering Mechanics* 1975; 101(4), 389-401.
29. Wen Y., K. Method for random vibration of hysteretic systems. *Journal of Engineering Mechanics* 1976; 102(2), 249-263.
30. Politopoulos, I., and Feau, C. Some aspects of floor spectra of 1DOF nonlinear primary structures. *Journal of Earthquake Engineering and Structural Dynamics*. 2007; 36:975–993.
31. Vanmarcke EH. *Structural response to earthquakes. Seismic Risk and Engineering Decisions*. Amsterdam: Elsevier, 1976.
32. Der Kiureghian A. Structural response to stationary excitation. *Journal of Engineering Mechanics*, ASCE, 1980; 106,1195-213.
33. Ricker, N. Further developments in the wavelet theory of seismogram structure. *Bull. Seism. Soc. Am* 1943; 33, 197-228.
34. Ricker N. Wavelet functions and their polynomials. *Geophysics* 1944;9, 314–323.
35. Vassiliou, M., F., and Makris, N. Estimating Time Scales and Length Scales in Pulselike Earthquake Acceleration Records with Wavelet Analysis. *Bull. Seism. Soc. Am*. 2011; 101(2), 596-618.
36. Baker, W.J., Quantitative classification of near fault ground motions using wavelet analysis, *Bull. Seism. Soc. Am.*, 2007; 97, 1486-1501.
37. Mavroeidis, G. P., A. S. Papageorgiou A mathematical representation of near-fault ground motions, *Bull. Seism. Soc. Am*. 2003; 93, 1099-1131.
38. Gabor, D., Theory of communication. I. The analysis of information, *IEEE* 1946;93, 429–441.